6-8-2014

Synthesis, spectroscopic, and cellular properties of α-pegylated cis-A_2B_2- and A_3B-types ZnPcs

Benson G. Ongarora
Louisiana State University

Zehua Zhou
Louisiana State University

Elizabeth A. Okoth
Louisiana State University

Igor Kolesnichenko
Louisiana State University

Kevin M. Smith
Louisiana State University

See next page for additional authors

Recommended Citation

Ongarora, B., Zhou, Z., Okoth, E., Kolesnichenko, I., Smith, K., & Vicente, M. (2014). Synthesis, spectroscopic, and cellular properties of α-pegylated cis-A_2B_2- and A_3B-types ZnPcs. *Journal of Porphyrins and Phthalocyanines, 18* (10-11), 1021-1033. https://doi.org/10.1142/S1088424614500849

HHS Public Access

Author manuscript

J Porphyr Phthalocyanines. Author manuscript; available in PMC 2015 June 08.

Published in final edited form as:

J Porphyr Phthalocyanines. 2014 ; 18(10-11): 1021–1033. doi:10.1142/S1088424614500849.

Synthesis, spectroscopic, and cellular properties of α-pegylated *cis*-A_2B_2- and A_3B-types ZnPcs

Benson G. Ongarora, **Zehua Zhou**, **Elizabeth A. Okoth**, **Igor Kolesnichenko**, **Kevin M. Smith**◆, and **M. Graça H. Vicente**[*,◆]

Department of Chemistry, Louisiana State University, Baton Rouge, LA 70803, USA

Abstract

A series of pegylated *cis*-A_2B_2- or A_3B-type ZnPcs, substituted on the α-positions with tri(ethylene glycol) and hydroxyl groups, were synthesized from a new bis-phthalonitrile. A clamshell-type bis-phthalocyanine was also obtained as a byproduct. The hydroxyl group of one ZnPc was alkylated with 3-dimethylaminopropyl chloride to afford a pegylated ZnPc functionalized with an amine group. All mononuclear ZnPcs were soluble in polar organic solvents, showed intense Q absorptions in DMF, and had fluorescence quantum yields in the range 0.10–0.23. The clamshell-type bis-phthalocyanine adopts mainly open shell conformations in DMF, and closed clamshell conformations in chloroform. All ZnPcs were highly phototoxic to human carcinoma HEp2 cells, particularly the amino-ZnPc mainly protonated under physiological conditions, which showed the highest phototoxicity (IC_{50} = 0.5 μM at 1.5 J/cm^2) and dark cytotoxicity (IC_{50} = 22 μM), in part due to its high cellular uptake. The ZnPcs localized in multiple organelles, including mitochondria, lysosomes, Golgi and ER.

Keywords

phthalocyanine; PEG; photosensitizer; cytotoxicity; cellular uptake

INTRODUCTION

Phthalocyanines (Pcs) are a class of tetrapyrrolic macrocycles related to the naturally occurring porphyrins; compared with the porphyrin ring, Pcs exhibit an extended 18 π-electron system with four benzene units fused onto the β-pyrrolic positions and nitrogen atoms at the *meso*-positions instead of the methine bridges in porphyrins [1, 2]. These structural features confer to Pcs a number of properties that make them highly desirable for a variety of applications in biology, medicine and materials science, including strong absorptions and emissions in the near-IR, high stability and easy macrocycle derivatization. Among their many current applications, Pcs have been used as blue-green colorant dyes, bioimaging agents, and as photosensitizers for the photodynamic therapy (PDT) or for the

[*]Correspondence to: M. Graça H. Vicente, vicente@lsu.edu, tel: +1 225-578-7405.

◆SPP full member in good standing

Dedicated to Professor Nagao Kobayashi on the occasion of his 65th birthday

photothermal therapy (PTT) of cancers [3–6]. PDT and PTT are minimally-invasive tumor treatments that involve activation of a tumor-localized photosensitizer with red light; in PTT the photoexcited molecules relax non-radiatively producing heat which induces cellular hyperthermia, whereas in PDT an excited triplet state sensitizer produces reactive oxygen species (ROS), such as $^1O_2$, which destroy cells *via* necrosis and/or apoptosis. Photofrin, a derivative of hematoporphyrin IX, has been used for nearly two decades for the PDT treatment of various cancers, including lung, skin, cervical and bladder [7–9]. Nevertheless, photofrin has some drawbacks because porphyrins typically absorb weakly in the red region of the spectrum, where light can penetrate deeper into tissues, and it tends to persist for long periods of time in healthy tissues, causing patient photosensitivity [10]. On the other hand, Pcs have been shown to be promising second-generation photosensitizers for PDT because of their intense absorptions in the near-IR (λ_{max} > 670 nm), their ability to cross cellular membranes and for producing ROS upon light activation [6]. Pcs in clinical use include Photosens, a tetrasulfonated Al(III) Pc, approved for the treatment of skin, breast, lung and gastrointestinal tract cancers [11, 12], a Si(IV)Pc known as Pc4 for the treatment of gliomas and breast, colon and ovarian cancers [13, 14], and ZnPc CGP55847 for the treatment of squamous cell carcinomas (SCC) of the upper aerodigestive tract [15, 16]. However, a drawback of metallo-Pcs is their intrinsic insolubility and tendency for aggregation in aqueous solutions, which can lead to a decrease or even loss of their photochemical activity. For this reason, various water-solubilizing peripheral substituents and/or axial ligands have been introduced into Pcs to minimize aggregation and increase their solubility in aqueous media; substituents include carboxylates, sulfonates, phosphonates, pyridinium ions, hydroxyl groups, peptides, carbohydrates, and polyethylene glycol (PEG) groups [6, 17–22]. Among these, the use of PEGs as delivery vehicles [23–25] or covalently bound to Pcs [19, 26–28] is a well-known strategy for improved delivery to target tissues, since PEG groups are demonstrated to increase water-solubility, serum life, cellular permeability and tumor accumulation of photosensitizers [29–32]. On the other hand, hydroxy-substituted Pcs are shown to have increased aqueous solubilities and enhanced photodynamic properties. As examples, Foscan/Temoporfin, a tetrahydroxyphenylchlorin [33, 34], and Lutex/Lutrin, a lutetium texaphyrin containing two short PEG chains and two hydroxyl groups [35, 36], have demonstrated higher photodynamic efficiency compared with Photofrin. Herein we report the synthesis, characterization and cellular properties of regioisomerically pure amphiphilic ZnPcs, of the *cis*-A_2B_2- and A_3B-types, containing one or two tri(ethylene glycol) groups on the α-position(s). We have previously shown that such short PEG groups possess lower conformational flexibility compared with larger PEGs, and therefore tend to minimize Pc aggregation, enhance fluorescence quantum yields and increase cellular uptake [18, 19, 37, 38]. In addition, these ZnPcs contain one or two hydroxyl groups or a dimethylamino functionality on the α-position(s); we have previously observed that ZnPcs substituted on the α- (rather than on the β-) positions tend to show higher phototoxicity [18, 39]. On the other hand, the zinc(II) ion was chosen due to its diamagnetic properties and the demonstrated ability of ZnPcs to generate singlet oxygen [18, 26, 39]. In order to prepare regioisomerically pure *cis*-A_2B_2-type ZnPc, we followed a methodology introduced by Kobayashi [40, 41] based on the use of a bis-phthalonitrile linked by a constrained bridging group; in contrast, the A_3B-type ZnPcs were obtained by condensation of two different

phthalonitriles, using an excess of unsubstituted phthalonitrile, as we have previously reported [19, 42].

RESULTS AND DISCUSSION

Synthesis and spectroscopic properties

The synthetic routes to di-pegylated *cis*-A_2B_2- type ZnPc **6** and mono-pegylated A_3B-type ZnPcs **9** and **10** are shown in Schemes 1 and 2, respectively. The precursor of all ZnPcs, phthalonitrile **1**, was prepared according to our previously published procedure, by reaction of 3,6-dihydroxyphthalonitrile with $CH_3(OCH_2CH_2)_3I$ [19]. With the goal to prepare regioisomerically pure *cis*-A_2B_2- type ZnPc, the bis-phthalonitrile **3** was synthesized in 84% yield, from the reaction of phthalonitrile **1** with 1,2-bis(bromomethyl)benzene **2** in DMF, in the presence of potassium carbonate. The bis-phthalonitrile **3**, bearing two tri(ethylene glycol) groups and a 1,2-(dihydroxymethyl) benzene protecting group [43–45], showed good solubility in organic solvents, which facilitated its purification and isolation. The reaction of bis-phthalonitrile **3** with various equivalents of phthalonitrile **4** (1–30 equiv) at 70–140 °C in dimethylaminoethanol (DMAE), in the presence of zinc(II) acetate and a catalytic amount of 1,5-diazabicyclo(4.3.0)non-5-ene (DBN) [18, 39], gave the A_2B_2-*adjacent* ZnPc **5** in up to 5% yield; ZnPcs **7** and **8** were also formed under the reaction conditions in 2–7% yields, similar to results previously published [44]. The formation of ZnPcs **7** and **8** in addition to **5** is a result of the higher flexibility of the 1,2-(dihydroxymethyl)benzene bridging group of **3** compared with the 2,2′-dihydroxy-1,1′-binaphthyl bridge previously reported [39–41, 46]. Deprotection of ZnPc **5** using concentrated H_2SO_4 [47] gave the dihydroxy-dipegylated ZnPc **6** in 95% yield, while under similar conditions a mixture of ZnPcs **7** and **8** gave the monohydroxy-monopegylated ZnPc **9** in 41% yield. The deprotection was performed at 0 °C for 15–30 min, to minimize demetalation of the ZnPcs; alternative deprotection conditions, including the use of HBr, BCl_3, or Pd(0)/H_2 gave lower yields of the targeted deprotected ZnPcs. ZnPc **9** could also be obtained directly from reaction of phthalonitrile **1** with **4**, in 6.8% yield, as previously reported [19, 42]. The O-alkylation of ZnPc **9** with 3-dimethylaminopropyl chloride afforded ZnPc **10** in 50% yield [48]. *N*-Demethylation of ZnPc **10** was not observed, even upon prolonged storage at room temperature, as has been reported for other *N*-methylated ZnPcs [39].

ZnPcs **6**, **9** and **10** showed good solubility in polar organic solvents, such as ethyl acetate, THF, DMF and DMSO, as well as in dichloromethane (DCM), facilitating their purification and isolation. However, none of the ZnPcs were soluble in water, even upon sonication, although all ZnPcs remained in aqueous solution when diluted from concentrated stocks in DMSO/Cremophor EL into phosphate buffer saline (final DMSO concentration of 1%, Cremophor EL 5%) up to 200 μM concentration (*vide infra*). The structures of all ZnPcs were confirmed by MALDI-TOF mass spectrometry and NMR spectroscopy. The regioisomerically pure ZnPcs show simplified ^{1}H NMR spectra compared with statistical mixtures of ZnPcs previously reported, obtained from cyclotetramerization of two mono-substituted phthalonitriles [18, 39]. The ^{1}H NMR spectrum of ZnPc **5** shows the characteristic OCH_2 protons of the 1,2-dimethylbenzene protecting group as a singlet at 6.42

ppm along with the benzene protons in the aromatic region, centered at 7.8 and 8.0 ppm. Removal of the protecting group under acidic conditions was confirmed by disappearence of these peaks from the ^{1}H NMR spectrum of ZnPc **6**. The ^{1}H NMR spectrum of ZnPc **6** shows the aromatic proton signals in the range 7.5– 9.3 ppm, the aliphatic protons on the PEG chains between 3.3–5.1 ppm, and the OH signals overlap with the solvent peak at around 3.5 ppm. Similarly, the bis-ZnPc **8** shows the Pc aromatic protons between 6.8–9.1 ppm, the OCH_2 protons of the protecting group at 7.01 ppm and the PEG proton signals between 3.3–4.8 ppm. Upon deprotection, the aromatic protons of A_3B-ZnPc **9** appear in the range 8.7–9.6 ppm and the PEG protons between 3.3–4.8 ppm. In addition to these peaks, the ^{1}H-NMR spectrum of ZnPc **10** also shows the two *N*-methyl groups as a singlet at 2.53 ppm and the methylene groups in the aliphatic region. ZnPcs **5**, **6**, **7**, **8**, **9** and **10** showed molecular ion peaks at *m/z* 1034.302, 932.294, 1163.369, 1614.396, 755.225 and 840.341, respectively, in their MALDI-MS.

The spectroscopic properties for ZnPcs **5**, **6**, **8**, **9** and **10** in DMF are summarized in Table 1 and their absorption spectra are shown in Fig. 1a. ZnPcs **5**, **9** and **10** show similar spectra with strong Q absorptions centered at about 690 nm, vibrational bands around 620 and 650 nm, and the Soret band centered at 340 nm. These ZnPcs show fluorescence emissions centered at about 693 nm, with small Stokes shifts (2–3 nm), and fluorescence quantum yields in the range 0.12–0.21, characteristic of non-aggregated ZnPcs [18, 39, 49]. On the other hand, ZnPc **6** shows broadened and red-shifted absorption bands, as well as lower fluorescence quantum yield, suggesting aggregation of this ZnPc in DMF. It is likely that upon deprotection of the 1,2-(dihydroxymethyl) benzene bridging group, the two hydroxyl groups of ZnPc **6** can be involved in intermolecular hydrogen bonding, leading to aggregation and fluorescence quenching. We have previously observed intermolecular hydrogen bonding in the X-ray crystal structure of phthalonitrile **1**, between the hydrogen of the OH group and an oxygen acceptor in the tri(ethylene glycol) chain [19].

The UV-vis spectrum of clamshell-type bis-ZnPc **8** shows a broadened and split Q-band in DMF, with λ_{max} centered at 640 and 687 nm of similar intensities, and the Soret band at 345 nm, suggesting mixed conformations in solution, mainly of the opened, or partially opened, clamshell-type [43–45, 50–53]. The UV-vis spectra of clamshell-type binuclear phthalocyanines have unique features as a result of conformational equilibria and of potential intramolecular interactions between the macrocycles. While the shape of the Q-band in the UV-vis spectrum obtained for ZnPc **8** in DMF (Fig. 1a) suggests opened shell conformations in this solvent, in chloroform the shape of the Q-band (Fig. 1b) and the observed quenching of the fluorescence suggest mainly closed clamshell conformations in this solvent. Upon addition of pyridine (1% vol) to the chloroform solution, a split Q-band similar to that seen in DMF solution is observed in the UV-vis spectrum of bis-ZnPc **8** (Fig. 1b), along with fluorescence enhancement, indicating that **8** again assumes mainly opened shell conformations in the presence of pyridine, as observed in DMF.

Cellular properties

The cellular properties of ZnPcs **5**, **6**, **8**, **9** and **10**, including the time-dependent cellular uptake, cytotoxicity and intracellular localization, were investigated in human carcinoma

HEp2 cells, and the results are summarized in Table 2 and in Figs 2–8. All ZnPcs showed low dark toxicity, with determined IC_{50} (50% inhibition of cell proliferation based on dose-response curves) > 200 μM, with the exception of ZnPc **10** which has a calculated IC_{50} value of 22 μM, using Promega's CellTiter Blue viability assay [18, 39]. Upon exposure to a low light dose (~1.5 J/cm^2), all ZnPcs were highly toxic to HEp2 cells, with calculated IC_{50} values between 0.5–14.5 μM (Fig. 2). The most toxic compound was ZnPc **10**, containing the amino functionality, which is mostly protonated under physiological conditions. This is not a surprising result, since we have previously observed high phototoxicity for mono-cationic porphyrin [54] and ZnPc [37], and in particular for cationic α-substituted ZnPcs [18, 39]. Such cationic photosensitizers can interact with negatively charged cell membranes and potentially target biomolecules such as DNA and RNA, resulting in effective photodamage and overall enhanced photodynamic efficacy. On the other hand, the neutral ZnPcs **5**, **6**, **8** and **9** showed much lower dark toxicity (IC_{50} > 200 μM) compared with the cationic ZnPc, lower phototoxicity (IC_{50} = 2–15 μM at 1.5 J/cm^2) and lower cellular uptake (*vide infra*). However, these ZnPcs were still highly phototoxic, in particular those containing two tri(ethylene glycol) groups, maybe due to increased electron density of the ring as a result of their α-substitution; we have previously observed high phototoxicity for *cis*-A_2B_2–type ZnPcs [39] and for α-substituted ZnPcs [18, 38].

The cationic ZnPc **10** accumulated the most within cells, and the fastest, at all time points investigated, probably due to its enhanced interactions with the negatively charged plasma membranes, enhancing its cellular uptake (Fig. 3). On the other hand, ZnPc **9** containing only one tri(ethylene glycol) and one hydroxyl group, was the least taken up by HEp2 cells at all times investigated, probably as a result of its lower aqueous solubility compared with the other ZnPcs [38]. The presence of the 1,2-(dihydroxymethyl)benzene group in ZnPc **5** did not alter its cellular uptake relative to that of the deprotected ZnPc **6**; on the other hand, bis-phthalocyanine **8** accumulated faster than **5** and **6** within cells, but after four hours the amount of ZnPcs **5**, **6** and **8** found in cells was similar. The subcellular distribution of ZnPcs **5**, **6**, **8**, **9** and **10** was investigated by fluorescence microscopy. The organelle-specific probes ER Tracker Blue/White (endoplasmic reticulum, ER), BODIPY Ceramide (Golgi), LysoSensor green (lysosomes) and MitoTracker green (mitochondria), were used in the co-localization experiments (the purple or yellow/orange colors indicate co-localization of ZnPc and organelle tracker in Figs 4–8). All ZnPcs localized in multiple organelles within the cells, namely the mitochondria, lysosomes, Golgi apparatus and ER. We have previously observed that pegylated and/or cationic ZnPcs can localize in the mitochondria, lysosomes, Golgi and ER [18, 37–39]. The high phototoxicity observed for this series of ZnPcs might be due to their localization in multiple organelles, which could lead to photodamage in several subcellular sites and to effective cell destruction.

EXPERIMENTAL

Synthesis

General—All reagents and solvents were purchased from commercial suppliers and used directly without further purification. Analytical thin-layer chromatography (TLC) was carried out using plastic backed TLC plates 254 (precoated, 200 μm) from Sorbent

Technologies. Silica gel 60 (230 × 400 mesh, Sorbent Technologies) was used for column chromatography. NMR spectra were recorded on a Liquid AV-400 Bruker spectrometer (400 MHz for ^{1}H, 100 MHz for ^{13}C). The chemical shifts are reported in δ ppm using the following incompletely deuterated solvents as internal references: CD_3COCD_3 2.04 ppm (^{1}H), 29.92 ppm (^{13}C); DMF-d_7 8.03 ppm (^{1}H), 163.15 ppm (^{13}C). MALDI-TOF mass spectra were recorded on a Bruker UltrafleXtreme (MALDI-TOF/TOF) instrument using 4-chloro-α-cyanocinnamic acid (CCA) as the matrix. Phthalonitrile **1** was synthesized according to the literature procedure [19].

Phthalonitrile 3—A mixture of **1**(1.592g, 5.2 mmol) and 1,2-bis(bromomethyl)benzene (**2**) (688.9 mg, 2.61 mmol) was dissolved in DMF (10 mL) and heated to 65 °C. Potassium carbonate (2.07 g, 0.015 mol) was added in four portions, 5 min apart. The reaction mixture was stirred for 4 h under argon at the same temperature. After cooling to room temperature, the mixture was poured into ice-cold water (100 mL) and filtered. The crude product was purified using an alumina column eluted with DCM/methanol (95:5) to give a light-yellow solid (1.57 g, 84.3%). ^{1}H NMR (acetone-d_6, 400 MHz): δ, ppm 7.71–7.61 (6H, m, Ar-H), 7.48–7.45 (2H, m, Ar-H), 5.57 (4H, s, OCH_2), 4.35 (4H, t, OCH_2), 3.87 (4H, t, OCH_2), 3.70–3.66 (4H, m, OCH_2), 3.60–3.55 (10H, m, OCH_2), 3.45 (4H, t, OCH_2), 3.27 (6H, s, OCH_3). ^{13}C NMR (acetone-d_6, 100 MHz): δ, ppm 156.6, 155.7, 135.1, 130.1, 129.9, 121.3, 121.0, 114.3, 114.1, 105.34, 105.28 (Ar-H), 72.7, 71.7, 71.3, 71.1, 71.0, 70.7, 70.2 (OCH_2), 58.9 (OCH_3). MS (MALDI-TOF): *m/z* 715.2981 and 737.2794 (calcd. for $[M + H]^+$ 715.2979 and $[M + Na]^+$ 737.2798).

Phthalocyanine 5—A mixture of phthalonitrile **3** (172.0 mg, 0.24 mmol), phthalonitrile **4** (845.6 mg, 6.60 mmol), and zinc(II) acetate (220.0 mg, 1.20 mmol) was dissolved in DMAE (13.0 mL). The mixture was heated at 140 °C under flow of argon, and one drop of DBN was added to the solution. The reaction mixture was further refluxed at 140 °C for 5 h. After the reaction, the solvent was removed under vacuum. The residue was dissolved in acetone and filtered under gravity to give a green viscous residue on concentration. A silica gel column eluted with DCM/methanol (95:5) separated the pegylated ZnPcs as a green fraction. A second silica gel column eluted with DCM/THF (3:1) gave ZnPc **5** as a green solid (12.7 mg, 5.1%.). ^{1}H NMR (DMF-d_7, 400 MHz): δ, ppm 9.28–9.17 (4H, m, Ar-H), 8.19–8.11 (4H, m, Ar-H), 8.02–7.95 (2H, m, Ar-H), 7.82–7.80 (2H, m, Ar-H), 7.71–7.63 (4H, m, Ar-H), 6.42 (4H, s, OCH_2), 4.95–4.48 (4H, m, OCH_2), 4.46 (4H, t, OCH_2), 4.10 (4H, t, OCH_2), 3.83 (4H, t, OCH_2), 3.65–3.56 (4H, m, OCH_2), 3.54–3.42 (4H, m, OCH_2), 3.24 (6H, s, OCH_3). ^{13}C NMR (DMF-d_7, 100 MHz): δ, ppm 155.1, 154.6, 154.3, 154.1, 153.8, 152.6, 150.9, 140.0, 139.5, 135.4, 134.7, 133.6, 133.0, 132.9, 130.4, 130.3, 130.0, 129.8, 129.1, 128.2, 126.2, 124.1, 124.0, 123.8, 123.5, 123.4, 122.7, 121.5, 116.7 (Ar-C), 76.6, 72.8, 72.0, 71.6, 71.5, 71.3, 71.2, 70.7, 70.4, 70.2 (OCH_2), 59.0 (OCH_3). MS (MALDI-TOF): *m/z* 1034.302 (calcd. for $[M]^+$ 1034.294). UV-vis (DMF): λ_{max}, nm (log ε) 340 (4.57), 629 (4.43), 697 (5.16).

Phthalocyanine 6—A solution of ZnPc **5** (22.5 mg, 21.7 mmol) in H_2SO_4 (5.0 mL) was stirred for 15 min at 0 °C and then poured into water/ice and extracted in a separatory funnel using DCM/methanol (9:1, 50.0 mL × 3). The combined organic extracts were washed with

2N $NaHCO_3$ (90.0 mL) and with water (5 mL × 2). The organic solvents were removed under reduced pressure and the resulting residue purified by column chromatography using mixed solvents, DCM/methanol (98:2 → 95:5 → 9:1) to give the title Pc as a green solid (19.2 mg, 95.0%). ^{1}H NMR (DMF-d_7, 400 MHz): δ, ppm 9.29 (4H, s, Ar-H), 8.17–7.95 (4H, m, Ar-H), 7.75–7.51 (4H, m, Ar-H), 5.06 (4H, br, OCH_2), 4.36 (4H, br, OCH_2), 4.09 (4H, t, OCH_2), 3.66 (4H, t, OCH_2), 3.51–3.43 (8H, m, OCH_2), 3.26 (6H, s, OCH_3). ^{13}C NMR (DMF-d_7, 100 MHz): δ, ppm 155.0, 154.2, 153.7, 151.5, 150.6, 149.8, 139.7, 139.4, 136.3, 130.0, 129.9, 124.0, 123.6, 123.2, 122.8, 119.8, 118.2 (Ar-C), 72.9, 72.8, 72.0, 71.6, 71.3, 71.2, 70.7 (OCH_2), 59.1, 59.0 (OCH_3). MS (MALDI-TOF): *m/z* 932.294 (calcd. for $[M]^+$ 932.247). UV-vis (DMF): λ_{max}, nm (log ε) 341 (4.86), 648 (4.63), 718 (5.23).

Phthalocyanines 7, 8—These ZnPcs were obtained as byproducts in the above synthesis of ZnPc **5**; ZnPc **7** was isolated (yield 4.4 mg, 1.6%) upon elution with chloroform and then DCM/methanol (92:2 → 95:5). MS (MALDI-TOF): *m/z* 1163.369 (calcd. for $[M + H]^+$ 1163.339). ZnPc **8** was purified using DCM/methanol (95:5) to afford a greenish solid (yield 28.2 mg, 7.3%). ^{1}H NMR (DMF-d_7, 400 MHz): δ, ppm 9.11–9.02 (7H, m, Ar-H), 8.53–8.41 (7H, m, Ar-H), 8.30–8.23 (4H, m, Ar-H), 8.17–8.08 (4H, m, Ar-H), 7.93–7.90 (2H, m, Ar-H), 7.82–7.77 (4H, m, Ar-H), 7.46–7.44 (2H, m, Ar-H), 7.01 (4H, s, OCH_2), 6.87–6.84 (2H, m, Ar-H), 4.65–4.55 (8H, m, OCH_2), 4.13–4.11 (4H, m, OCH_2), 3.89–3.86 (4H, m, OCH_2), 3.73–3.70 (4H, m, OCH_2), 3.55–3.52 (4H, m, OCH_2), 3.30 (6H, s, OCH_3). ^{13}C NMR (DMF-d_7, 100 MHz): δ, ppm 154.1, 153.5, 152.9, 152.4, 152.3, 151.8, 151.1, 150.6, 150.4, 140.4, 139.6, 139.4, 139.2, 139.0, 137.8, 130.2, 130.0, 129.2, 129.1, 129.4, 129.0, 128.2, 126.7, 126.3, 123.6, 123.34, 123.26, 123.0, 122.7, 119.2, 118.7, 117.4, 114.4 (Ar-C), 73.5, 72.9, 72.1, 72.0, 71.7, 71.6, 71.5, 71.4, 69.5 (OCH_2), 59.1 (OCH_3). MS (MALDI-TOF): *m/z* 1633.403 (calcd. for $[M + Na]^+$ 1633.363). UV-vis (DMF): λ_{max}, nm (log ε) 336 (4.93), 638 (5.01), 687 (4.98).

Phthalocyanine 9—This Pc was obtained as previously reported [19]. Alternatively, ZnPc **8** (22.5 mg, 13.9 mmol) was dissolved in H_2SO_4 (5.0 mL) and stirred at 0 °C for 30 min. The mixture was poured into ice/water and extracted in a separatory funnel using DCM/methanol (9:1, 50.0 mL). The organic extracts were washed with 2N $NaHCO_3$ until neutral pH, then washed with water (5 mL × 2). The organic solvents were removed under reduced pressure and the residue purified by silica gel column chromatography eluted with DCM/ethyl acetate (1:2) to give Pc **9** as a greenish solid (10.1 mg, 41.0%). ^{1}H NMR (DMF-d_7, 400 MHz): δ, ppm 9.32–9.02 (6H, m, Ar-H), 8.29–8.12 (6H, m, Ar-H), 7.82–7.42 (2H, m, Ar-H), 6.9 (1H, br, OH), 5.11–4.97 (2H, m, OCH_2), 4.45–4.42 (2H, m, OCH_2), 4.12 (2H, t, OCH_2), 3.68 (4H, br, OCH_2), 3.48 (2H, t, OCH_2), 3.27 (3H, s, OCH_3). ^{13}C NMR (DMF-d_7, 100 MHz): δ, ppm 154.4, 153.9, 152.9, 150.7, 139.3, 138.0, 130.3, 130.2, 129.4, 126.7, 123.8, 123.5, 123.4, 123.2, 123.0, 119.7, 117.7 (Ar-C), 72.9, 72.1, 71.7, 71.4 (OCH_2), 59.1 (OCH_3). MS (MALDI-TOF) *m/z* 755.225 (calcd. for $[M]^+$ 755.171). UV-vis (DMF): λ_{max}, nm (log ε) 342 (4.71), 628 (4.49), 694 (5.19).

Phthalocyanine 10—ZnPc **9** (18.1 mg, 0.024 mmol) and 3-(dimethylamino)propyl chloride hydrochloride (4.7 mg, 0.030 mmol) were dissolved in DMF (5.0 mL) [48]. The solution was heated at 80 °C under argon, and K_2CO_3 (50.0 mg, 3.6 mmol) was added to the

reaction solution. The mixture was heated at 65 °C for 6 h. The solvent was removed under reduced pressure and the residue dissolved in DCM/methanol (9:1, 5.0 mL). The mixture was diluted with ethyl acetate, washed with water (20 mL) and dried to give a blue solid. The solid residue was purified by silica gel column chromatography using DCM/methanol (9:1) for elution to give Pc **10** as a blue-green solid (10.0 mg, 49.8%). ^{1}H NMR (DMF-d_7, 400 MHz): δ, ppm 9.52–9.45 (8H, m, Ar-H), 8.27–8.19 (6H, m, Ar-H), 5.03 (2H, t, OCH_2), 4.82 (2H, t, OCH_2), 4.49 (2H, t, OCH_2), 4.11 (2H, t, OCH_2), 3.84 (2H, t, OCH_2), 3.67–3.65 (2H, m, OCH_2), 3.47 (2H, t, CH_2), 3.34–3.28 (2H, m, CH_2), 3.25 (3H, s, OCH_3), 2.66–2.60 (2H, m, CH_2), 2.53 (6H, s, $N(CH_3)_2$). ^{13}C NMR (DMF-d_7, 100 MHz): δ, ppm 154.9, 154.8, 154.7, 154.5, 154.2, 152.3, 151.6, 140.3, 140.0, 130.1, 130.0, 129.3, 128.7, 123.8, 123.4, 123.4, 123.3, 117.9, 116.2 (Ar-C), 72.8, 72.0, 71.6, 71.3, 68.9 (OCH_2), 59.0 (OCH_3), 57.8 (*N*-CH_2), 45.9 ($N(CH_3)_2$), 28.9 (CH_2). MS (MALDI-TOF): *m/z* 840.341 (calcd. for $[M + H]^+$ 840.260). UV-vis (DMF): λ_{max}, nm (log ε) 341 (4.51), 624 (4.28), 690 (5.00).

Spectroscopic studies

All absorption spectra were measured on a UV-vis NIR scanning spectrometer UV-3101PC SHIMADZU equipped with a CPS-260 lamp. Stock solutions (1000 μM, 1.0 mL) of all ZnPcs were prepared in DMF (HPLC grade) and the dilutions achieved by spiking 20–80 μL of the corresponding stock solution into DMF to a 10.0 mL final volume. Emission spectra were recorded on a Fluorolog®-HORIBA JOBINVYON (Model LFI-3751) spectrofluorimeter. The optical densities of the solutions used for emission studies remained between 0.04–0.05 (AU) at the excitation wavelengths for all the ZnPcs. All experiments were carried out within 3 h of solution preparation at room temperature (23–25 °C) using a 10 mm path length spectrophotometric cell. The fluorescent quantum yields (Φ_f) were determined using a secondary standard method and unsubstituted ZnPc ($\Phi_f = 0.17$) as the reference [39, 55].

Cell studies

General—The HEp2 cell line used in this study was purchased from ATCC. The culture medium and reagents were purchased from Life Technologies. The HEp2 cells were cultured in medium (DMEM:Advanced = 1:1) containing 10% FBS and 1% antibiotic (penicillin-streptomycin). Stock solutions of each ZnPc at 32 mM concentration were prepared by dissolving the ZnPc in 96% DMSO and 4% Cremophor EL. Then, 2 mL of 400 μM compound solutions containing 1.95% DMSO and 0.05% Cremophor EL were prepared by adding 15 μL DMSO, and 25 μL of the 32 mM compound stock into 1960 μL medium. These solutions were sonicated for 5 min and used immediately, without filtration.

Dark cytotoxicity—The HEp2 cells at 15000 cells per well were plated in a Costar 96-wellplate(BDbiosciences) and grown overnight. The cells were exposed to different concentrations of ZnPc 200, 100, 50, 25, 12.5, and 0 μM, five repetitions for each concentration, and incubated at 37 °C. After 24 h incubation, excess ZnPc was removed by washing cells with 1X PBS and replaced with medium containing 20% Cell Titer Blue. The cells were incubated for an additional 4 h at 37 °C. The viable cells were measured fluorescently at 570/615 nm using a FluoStar Optima micro-plate reader. The dark toxicity is expressed in terms of the percentage of viable cells.

Phototoxicity—ZnPc concentrations of 50, 25, 12.5, 6.25, 3.125, and 0 μM were used for the phototoxicity experiments. The HEp2 cells were placed in 96 well plates as described above, and treated with ZnPc for 24 h at 37 °C. After 24 h treatment, the loading media was removed. The cells were washed with medium, and then refilled with fresh medium. The cells were then exposed to a 600 W halogen lamp light filtered through a water filter (Newport) and then through a beam turning mirror (200–3000 nm, Newport) to generate an approximate light dose of 1.5 J/cm^2. After a 20 min exposure time, the cells were incubated for another 24 h. After 24 h incubation, the medium was removed and replaced with medium containing 20% Cell Titer Blue. The cells were incubated for an additional 4 h. The viable cells were measured fluorescently at 570/615 nm using a FluoStar Optima micro-plate reader. The phototoxicity was expressed in terms of the percentage of viable cells.

Time-dependent cellular uptake—The HEp2 cells were plated at 15,000 cells per well in a Costar 96-well plate (BD biosciences) and grown overnight. The 10 μM ZnPc working concentration was made by diluting 400 μM stock solution with medium containing 5% FBS and 1% antibiotic. The cells were treated by adding 100 μL per well of 10 μM working solution at different time periods of 0, 1, 2, 4, 8, and 24 h. The loading medium was removed at the end of the treatments. The cells were washed with 1X PBS, and solubilized by adding 0.25% Triton X-100 in 1X PBS. A ZnPc standard curve of 10 μM, 5 μM, 2.5 μM, 1.25 μM, 0.625 μM and 0.3125 μM was performed by diluting 400 μM ZnPc solution with 0.25% Triton X-100 (Sigma-Aldrich) in 1X PBS. A cell standard curve was prepared using 10,000, 20,000, 40,000, 60,000, 80,000, and 10,000 cells per well. The cells were quantified using the CyQuant Cell Proliferation Assay (Life Technologies). The amount of ZnPc and cell numbers were determined using a FluoStar Optima micro-plate reader (BMG LRBTEH), and the wavelengths 355/700 nm for ZnPc and 570/615 nm for cells, respectively.

Microscopy—The HEp2 cells were placed in six well plates, allowed to grow overnight, and then exposed to 10 μM concentration of ZnPc for 6 h. After exposure to ZnPc, the following organelle tracers were added: LysoSensor Green 50 nM, MitoTracker Green 250 nM, ER Tracker Blue/white 100 nM, and BODIPY FL C5 Ceramide 50 nM. The organelle tracers were added to the medium and the cells were incubated concurrently with the ZnPc and the tracer for 30 min. The cells were washed with 1X PBS three times, and then refilled 1X PBS 5 mL/well. The subcellular distribution of compounds were determined by using a Zeiss AxioVert 200 M inverted fluorescence microscope fitted with standard GFP, DAPI, and Cy5 filter sets.

CONCLUSIONS

The synthesis of regioisomerically pure *cis*-A_2B_2-ZnPcs is described from a bisphthalonitrile containing a 1,2-(dihydroxymethyl)benzene bridge and two tri(ethylene glycol) groups. A clamshell-type bis-ZnPc and a A_3B-type ZnPc were also obtained as side products from this reaction. Deprotection of the 1,2-(dihydroxymethyl) benzene group produced the corresponding α-pegylated and α-hydroxy ZnPcs. The A_3B-type ZnPc was also prepared by condensation of two different phthalonitriles, using a large excess of unsubstituted phthalonitrile. The α-hydroxyl group of ZnPc **9** was alkylated using 3-

dimethylaminopropyl chloride to afford the corresponding mono-amino-ZnPc. Pegylation of the macrocycles significantly improved the solubility of the ZnPcs and facilitated their purification. While in DMF ZnPcs **5**, **9** and **10** show UV-vis and emission spectra typical of monomeric Pcs in solution, under similar conditions ZnPc **6** shows aggregation and the lowest fluorescence quantum yield of all ZnPcs investigated. On the other hand, the spectra obtained for the clamshell-type bis-phthalocyanine **8** is significantly different from all other ZnPcs; in DMF, bis-ZnPc adopts open or partially open shell conformations, while in chloroform it adopts mainly closed clamshell conformations.

The most phototoxic ZnPc was the amino-ZnPc **10**, mainly protonated under physiological conditions, which was found to have IC_{50} = 0.5 μM at 1.5 J/cm^2; this ZnPc also accumulated the most within human carcinoma HEp2 cells of all ZnPcs investigated, likely due to enhanced interactions with membrane-containing phosphate groups in comparison with the neutral ZnPcs. On the other hand, α-mono-hydroxyl ZnPc **9** was the least phototoxic (IC_{50} = 14.5 μM at 1.5 J/cm^2) and accumulated the least within cells, in part due to its lower aqueous solubility. All ZnPcs localized preferentially in mitochondria, lysosomes, Golgi and ER, suggesting that photodamage in multiple sites could result from light activation of these ZnPcs, leading to effective cell destruction.

Acknowledgments

The work described was supported by the US National Institutes of Health (grant no. R01 CA179902).

References

1. Leznoff, CC.; Lever, ABP., editors. Phthalocyanines: Properties and Applications. Vol. 1–4. VCH Publishers; 1989, 1993, 1996.
2. McKeown, NB. The Porphyrin Handbook: The synthesis of symmetrical phthalocyanines. Kadish, KM.; Smith, KM.; Guilard, R., editors. Vol. 15. Academic Press; Boston: 2003. p. 98-124.
3. Erk, P.; Hengelsberg, H. The Porphyrin Handbook: Phthalocyanines dyes and pigments. Kadish, KM.; Smith, KM.; Guilard, R., editors. Vol. 19. Academic Press; Boston: 2003. p. 106-146.
4. Ben-Hur, E.; Chan, W-S. The Porphyrin Handbook: Phthalocyanines in photobiology and their medical applications. Kadish, KM.; Smith, KM.; Guilard, R., editors. Vol. 19. Academic Press; Boston: 2003. p. 1-35.
5. Lim C-K, Shin J, Lee Y-D, Kim J, Oh KS, Yuk SH, Jeong SY, Kwon IC, Kim S. Theranostics. 2012; 2:871–879. [PubMed: 23082099]
6. Josefsen LB, Boyle RW. Theranostics. 2012; 2:916–966. [PubMed: 23082103]
7. Huang Z. Tech Cancer Res Treatment. 2005; 4:283–293.
8. Brown SB, Brown EA, Walker I. Lancet Oncol. 2004; 5:497–508. [PubMed: 15288239]
9. Detty MR, Gibson SL, Wagner SJ. J Med Chem. 2004; 47:3897–3915. [PubMed: 15267226]
10. Pandey, RK.; Zheng, G. The Porphyrin Handbook: Porphyrins as Photosensitizers in Photodynamic Therapy. Kadish, KM.; Smith, KM.; Guilard, R., editors. Vol. 6. Academic Press; Boston: 2000. p. 157-230.
11. Zharkova NN, Kozlov DN, Smirnov VV, Sokolov VV, Chissov VI, Filonenko EV, Sukhin GM, Galpern MG, Vorozhtsov GN. Proc SPIE. 1995; 2325:400–403.
12. Sokolov VV, Chissov VI, Yakubovskya RI, Aristarkhova EI, Filonenko EV, Belous TA, Vorozhtsov GN, Zharkova NN, Smirnov VV, Zhitkova MB. Proc SPIE. 1996; 2625:281–287.
13. Kinsella TJ, Baron ED, Colussi VC, Cooper KD, Hoppel CL, Ingalls ST, Kenney ME, Li X, Oleinick NL, Stevens SR, Remick SC. Front Oncol. 2011; 14:1–6.

14. Baron ED, Malbasa CL, Santo-Domingo D, Fu P, Miller JD, Hanneman KK, Hsia AH, Oleinick NL, Colussi VC, Cooper KD. Lasers Surg Med. 2010; 10:728–735. [PubMed: 21246576]
15. Ochsner M. J Photochem Photobiol, B. 1996; 32:3–9. [PubMed: 8725049]
16. Fabris C, Soncin M, Miotto G, Fantetti L, Chiti G, Dei D, Roncucci G, Jori G. J Photochem Photobiol, B. 2006; 83:48–54. [PubMed: 16427302]
17. Dumoulin F, Durmus M, Ahsen V, Nyokong T. Coord Chem Rev. 2010; 254:2792–2847.
18. Ongarora BG, Hu X, Verberne-Sutton D, Garno JC, Vicente MGH. Theranostics. 2012; 2:850–870. [PubMed: 23082098]
19. Li H, Fronczek FR, Vicente MGH. Tetrahedron Lett. 2011; 52:6675–6678. [PubMed: 22505781]
20. Li H, Fronczek FR, Vicente MGH. J Med Chem. 2008; 51:502–511. [PubMed: 18189349]
21. Li H, Nguyen N, Fronczek FR, Vicente MGH. Tetrahedron. 2009; 65:3357–3363.
22. Lafont D, Zorlu Y, Savoie H, Albrieux F, Ahsen V, Boyle RW, Dumoulin F. Photodiag Photodyn Ther. 2013; 10:252–259.
23. Gijsens A, Derycke A, Missiaen L, De Vos D, Huwyler J, Eberle A, de Witte P. Int J Cancer. 2002; 101:78–85. [PubMed: 12209592]
24. Arnida NN, Kanayama N, Jang W-D, Yamasaki Y, Kataoka K. J Controlled Release. 2006; 115:208–215.
25. Suzuki T, Oishi M, Nagasaki Y. J Photopoly Sci Tech. 2009; 22:547–550.
26. Bai M, Lo P-C, Ye J, Wu C, Fong W-P, Ng DKP. Org Biomol Chem. 2011; 9:7028–7032. [PubMed: 21858322]
27. Durmus M, Ayhan MM, Gürek AG, Ahsen V. Dyes Pigm. 2008; 77:570–577.
28. Tuncel S, Dumoulin F, Gailer J, Sooriyaarachchi M, Atilla D, Durmus M, Bouchu D, Savoie H, Boyle RW, Ahsen V. Dalton Trans. 2011; 40:4067–4079. [PubMed: 21152655]
29. Fang J, Sawa T, Akaike T, Greish K, Maeda H. Int J Cancer. 2004; 109:1–8. [PubMed: 14735461]
30. Ichikawa K, Hikita T, Maeda N, Takeuchi Y, Namba Y, Oku N. Biol Pharm Bull. 2004; 27:443–444. [PubMed: 14993821]
31. Krueger T, Altermatt HJ, Mettler D, Scholl B, Magnusson L, Ris HB. Lasers Surg Med. 2003; 32:61–68. [PubMed: 12516073]
32. Rovers JP, Saarnak AE, De Jode M, Sterenborg HJ, Terpstra OT, Grahn MF. Photochem Photobiol. 2000; 71:211–217. [PubMed: 10687396]
33. Kübler AC, Haase T, Staff C, Kahle B, Rheinwald M, Mühling J. Laser Surg Med. 1999; 25:60–68.
34. Moore CM, Nathan TR, Lees WR, Mosse CA, Freeman A, Emberton M, Bown SG. Laser Surg Med. 2006; 38:356–363.
35. Zhu TC, Finlay JC, Hahn SM. J Photochem Photobiol, B. 2005; 79:231–241. [PubMed: 15896650]
36. Verigos K, Stripp DCH, Mick R, Zhu TC, Whittington R, Smith D, Dimofte A, Finlay J, Busch TM, Tochner ZA, Malkowicz SB, Glatstein E, Hahn SM. J Environ Path Tox Oncol. 2006; 25:373–387.
37. Sibrian-Vazquez M, Ortiz J, Nesterova, Fernández-Lázaro F, Sastre-Santos A, Soper SA, Vicente MGH. Bioconjugate Chem. 2007; 18:410–420.
38. Ongarora BG, Fontenot KR, Hu X, Sehgal I, Satyanarayana-Jois SD, Vicente MGH. J Med Chem. 2012; 55:3725–3738. [PubMed: 22468711]
39. Ongarora BG, Hu X, Li H, Fronczek FR, Vicente MGH. Med Chem Commun. 2012; 3:179–194.
40. Kobayashi N, Miwa H, Isago H, Tomura T. Inorg Chem. 1999; 38:479–485. [PubMed: 11673952]
41. Kobayashi N, Miwa H, Nemykin VN. J Am Chem Soc. 2002; 124:8007–8020. [PubMed: 12095345]
42. Li H, Fronczek FR, Vicente MGH. Tetrahedron Lett. 2008; 49:4828–4830.
43. Tolbin AY, Ivanov AV, Tomilova LG, Zefirov NS. Mendeleev Commun. 2002; 3:96–97.
44. Tolbin AY, Ivanov AV, Tomilova LG, Zefirov NS. J Porphyrins Phthalocyanines. 2003; 7:162–166.
45. Tolbin AY, Pushkarev VE, Shulishov EV, Tomilova LG. J Porphyrins Phthalocyanines. 2012; 16:341–350.

46. Seotsanyana-Mokhosi I, Nyokong T. J Porphyrins Phthalocyanines. 2005; 9:476–483.
47. Tolbin AY, Tomilova LG. Mendeleev Commun. 2008; 18:286–288.
48. Merkas S, Litvic M, Cepanec I, Vinkovic V. Molecules. 2005; 10:1429–1437. [PubMed: 18007539]
49. Ishii, K.; Kobayashi, N. The Porphyrin Handbook: The photophysical properties of phthalocyanines and related compounds. Kadish, KM.; Smith, KM.; Guilard, R., editors. Vol. 16. Academic Press; Boston: 2003. p. 1-42.
50. Yoshiyama H, Shibata N, Sato T, Nakamura S, Toru T. Org Biomol Chem. 2008; 6:4498–4501. [PubMed: 19039355]
51. Gonzalez A, Vazquez P, Torres T. Tetrahedron Lett. 1999; 40:3263–3266.
52. Leznoff CC, Drew DM. Can J Chem. 1996; 74:307–318.
53. Seotsanyana-Mokhosi I, Maree S, Maree MD, Nyokong T. J Porphyrins Phthalocyanines. 2003; 7:167–175.
54. Jensen TJ, Vicente MGH, Luguya R, Norton J, Fronczek FR, Smith KM. J Photochem Photobiol, B. 2010; 100:100–111. [PubMed: 20558079]
55. Zorlu Y, Dumoulin F, Durmus M, Ahsen V. Tetrahedron. 2010; 66:3248–3258.

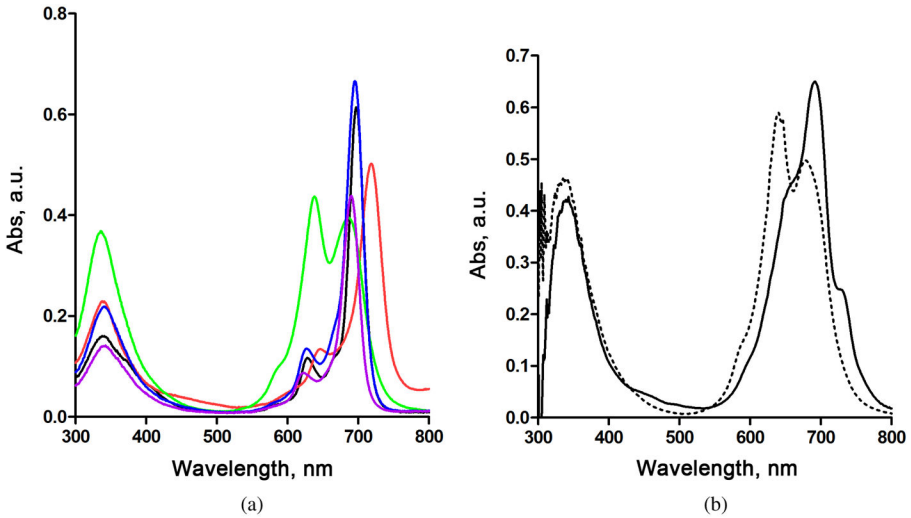

Fig. 1.

Absorption spectra for (a) ZnPc **5** (black), **6** (red), **8** (green), **9** (blue), and **10** (purple) in DMF, and (b) ZnPc **8** in chloroform (full line) and in 1% vol pyridine in chloroform (dashed line), at 4 μM concentration

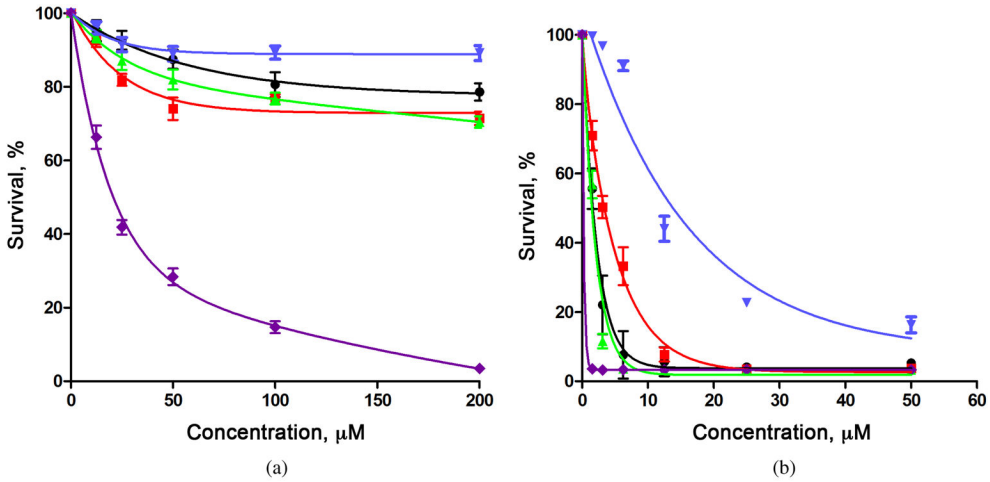

Fig. 2.

(a) Dark toxicity of ZnPc **5** (black), **6** (red), **8** (green), **9** (blue), and **10** (purple) toward HEp2 cells, using the Cell Titer Blue assay. (b) Phototoxicity of ZnPc **5** (black), **6** (red), **8** (green), **9** (blue), and **10** (purple) toward HEp2 cells, using the Cell Titer Blue assay

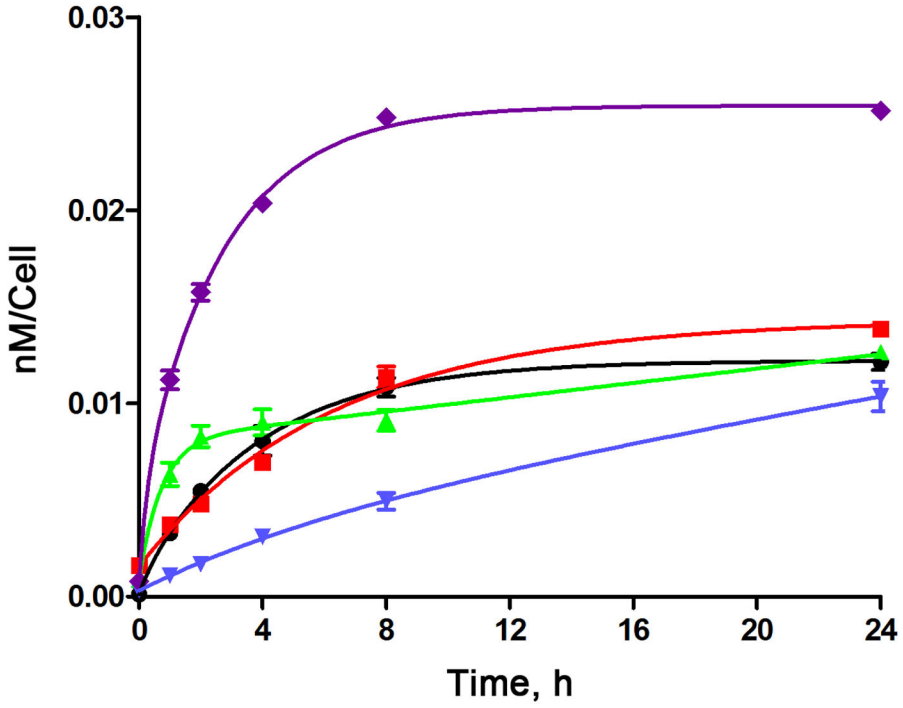

Fig. 3.

Time-dependent uptake of ZnPcs **5** (black), **6** (red), **8** (green), **9** (blue), and **10** (purple) at 10 μM toward HEp2 cells.

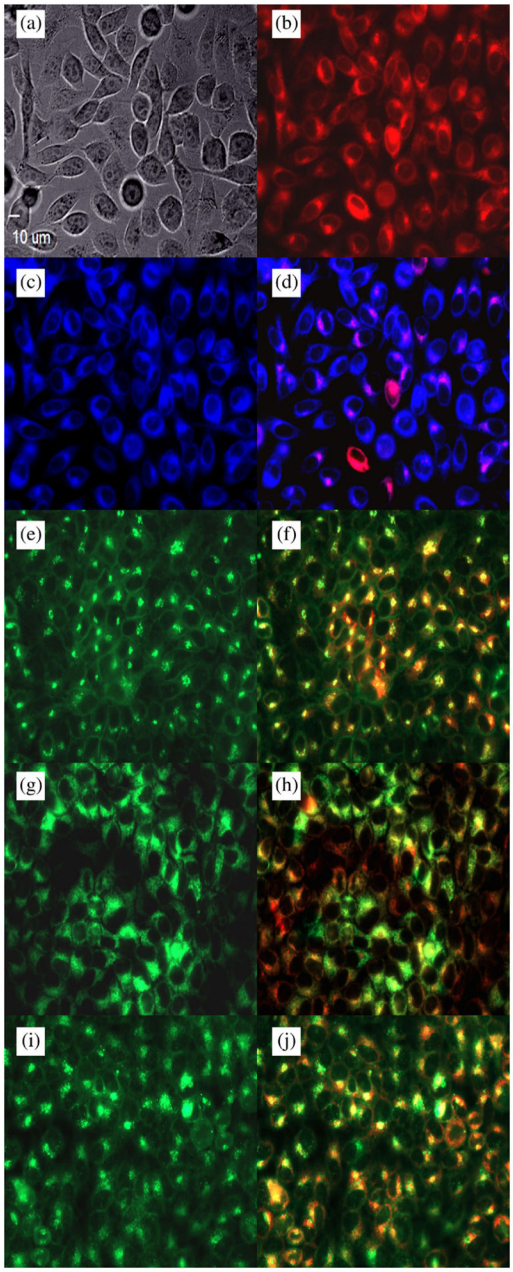

Fig. 4.

Subcellular localization of Pc **5** in HEp2 cells at 10 μM for 6 h. (a) Phase contrast, (b) Pc **5** fluorescence, (c) ER Tracker Blue/White fluorescence, (e) MitoTrack green fluorescence, (g) BODIPY Ceramide, (i) LysoSensor green fluorescence, and (d, f, h, j) overlays of organelle tracers with **5** fluorescence. Scale bar: 10 μm

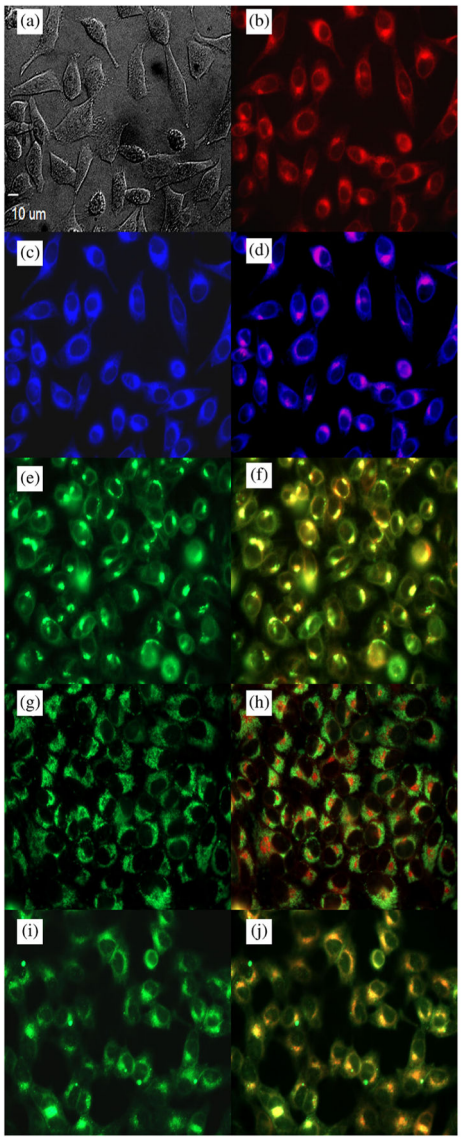

Fig. 5.

Subcellular localization of Pc **6** in HEp2 cells at 10 μM for 6 h. (a) Phase contrast, (b) Pc **6** fluorescence, (c) ER Tracker Blue/White fluorescence, (e) MitoTrack green fluorescence, (g) BODIPY Ceramide, (i) LysoSensor green fluorescence, and (d, f, h, j) overlays of organelle tracers with **6** fluorescence. Scale bar: 10 μm

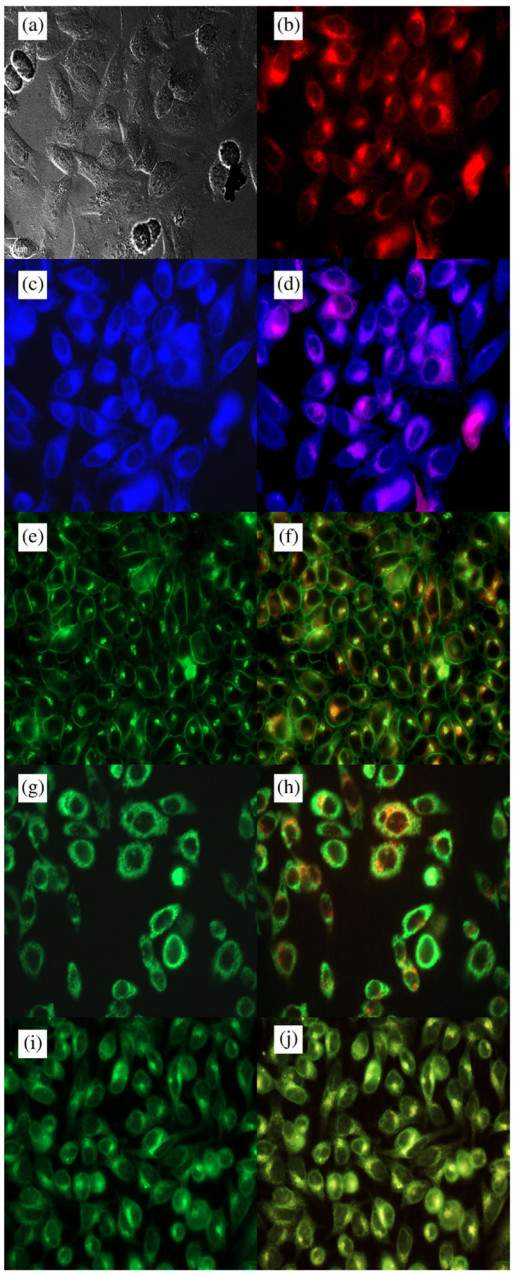

Fig. 6.

Subcellular localization of Pc **8** in HEp2 cells at 10 μM for 6 h. (a) Phase contrast, (b) Pc **8** fluorescence, (c) ER Tracker Blue/White fluorescence, (e) MitoTrack green fluorescence, (g) BODIPY Ceramide, (i) LysoSensor green fluorescence, and (d, f, h, j) overlays of organelle tracers with **8** fluorescence. Scale bar: 10 μm

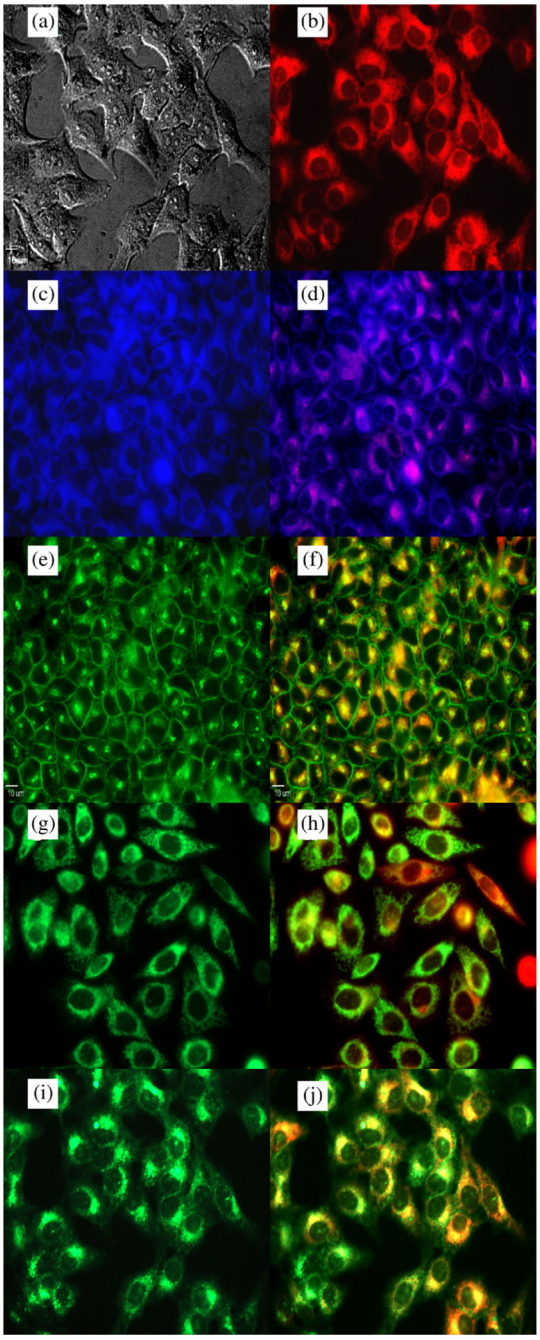

Fig. 7.

Subcellular localization of Pc **9** in HEp2 cells at 10 μM for 6 h. (a) Phase contrast, (b) Pc **9** fluorescence, (c) ER Tracker Blue/White fluorescence, (e) MitoTrack green fluorescence, (g) BODIPY Ceramide, (i) LysoSensor green fluorescence, and (d, f, h, j) overlays of organelle tracers with **9** fluorescence. Scale bar: 10 μm

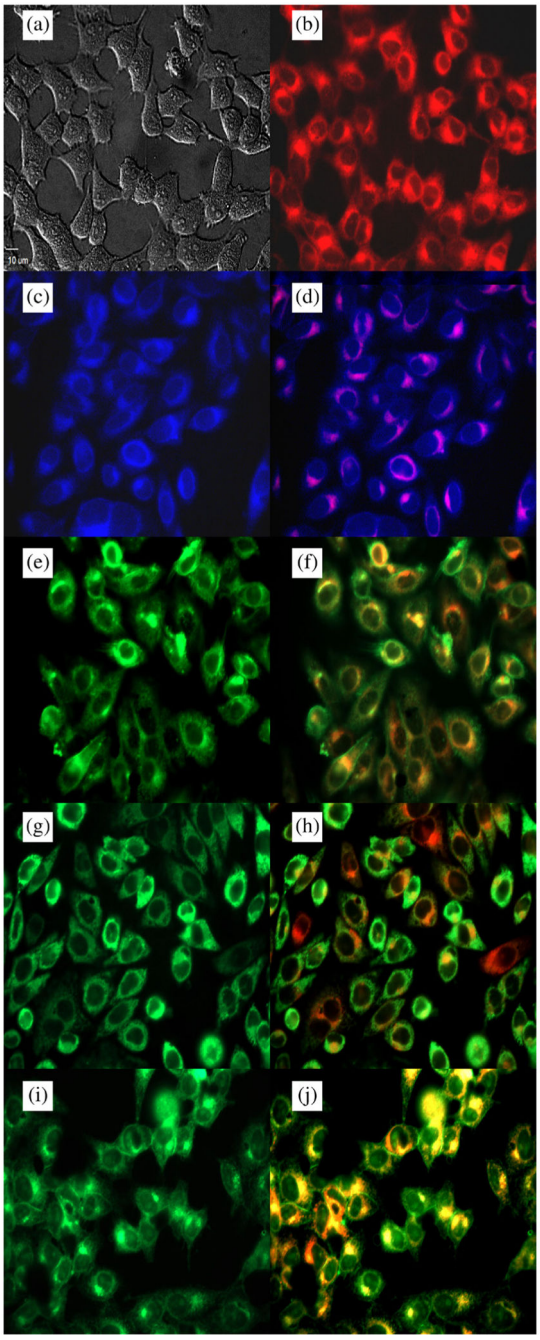

Fig. 8.

Subcellular localization of Pc **10** in HEp2 cells at 10 μM for 6 h. (a) Phase contrast, (b) Pc **10** fluorescence, (c) ER Tracker Blue/White fluorescence, (e) MitoTrack green fluorescence, (g) BODIPY Ceramide, (i) LysoSensor green fluorescence, and (d, f, h, j) overlays of organelle tracers with **10** fluorescence. Scale bar: 10 μm

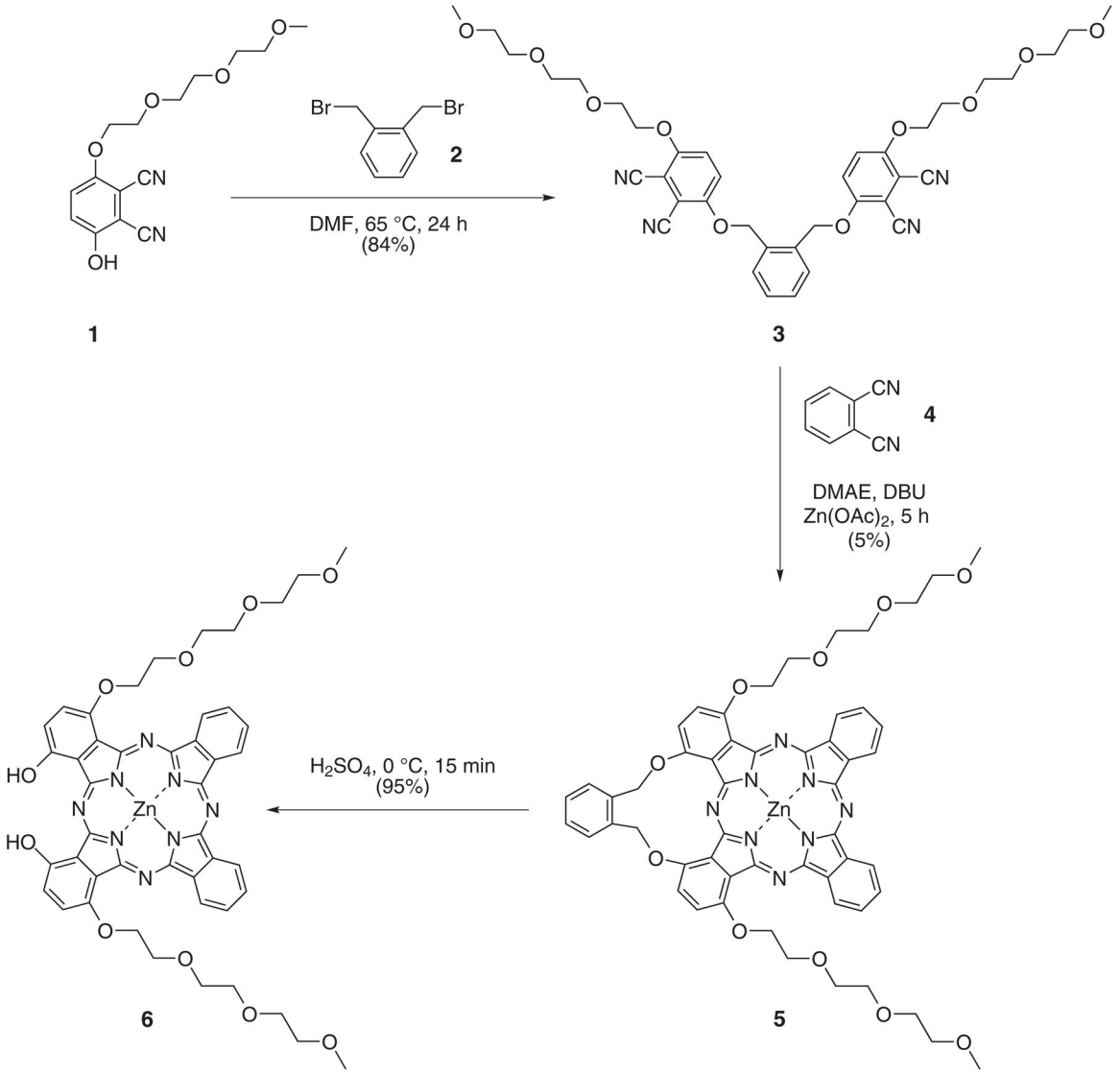

Scheme 1.

Synthetic route to *cis*-A_2B_2-type phthalocyanine **5**

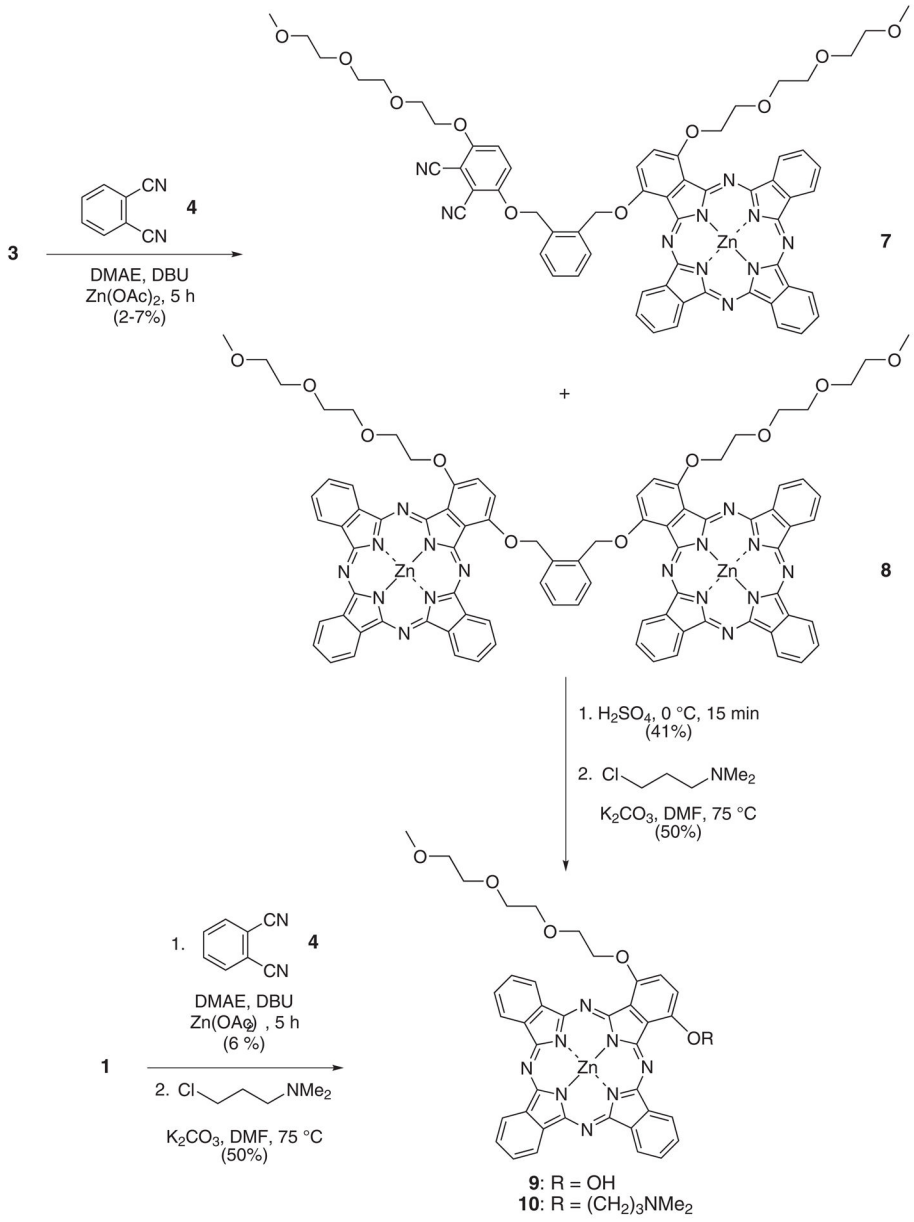

Scheme 2.

Synthetic route to A_3B-type phthalocyanines **9** and **10**

Table 1

Spectroscopic data for ZnPc **5**, **6**, **8**, **9** and **10** in DMF at room temperature

ZnPc	Absorption (λ_{max}, nm)	Emission[a] (λ_{max}, nm)	Stokes' shift, nm	Φ_F[b]
5	697	700	3	0.12
6	718	722	4	0.10
8	687	697	10	0.23
9	694	696	2	0.14
10	690	693	3	0.21

[a] Excitation at 640 nm;

[b] calculated using ZnPc as standard.

Table 2

Cytotoxicity (CellTiter Blue assay, light dose ~1.5 J/cm^2) and preferential localization sites for ZnPcs using human HEp2 cells

ZnPc	Dark toxicity IC_{50}, μM	Phototoxicity IC_{50}, μM	Sites of major (+++) and minor (+) subcellular localization
5	>200	2.0	Mitochondria (+++), Lysosomes (+++), Golgi (+++), ER (++)
6	>200	4.0	Mitochondria (+++), Lysosomes (+++), Golgi (+++), ER (++)
8	>200	2.0	Mitochondria (++), Lysosomes (+++), Golgi (++), ER (+++)
9	>200	14.5	Mitochondria (++), Lysosomes (+++), Golgi (++), ER (+++)
10	22.0	0.5	Mitochondria (+), Lysosomes (+++), Golgi (+++), ER (+++)